Methodology for Analyzing Dissolved Oxygen Consumption in Benthic Chambers

Alberto de la Fuente, Ph.D.[1]

Abstract: Dissolved oxygen (DO) consumption in the sediments of natural aquatic ecosystems occurs by mass flux across the water-sediment interface. This mass flux is determined as either the rate of oxygen consumption in the sediment or the rate of DO diffusion across the diffusive sublayer. The thickness of the diffusive sublayer is determined by the flow conditions in the turbulent water column. Consequently, feedback occurs between the biochemical consumption that occurs in the sediment and the flow that occurs in the water column. Together, these conditions define the DO flux across the water-sediment interface. Benthic chambers have been used to measure this flux in field and experimental conditions. However, these measurements do not account either for the fact that the flow inside a benthic chamber is not representative of field conditions or for the DO consumption in the water column. Thus, they can provide an inaccurate estimation of the sediment DO demanded in the field. This article aims to present and discuss an approach for analyzing a time series of DO depletion inside a benthic chamber. Based on this approach, the processes related to turbulent water transport in the column are separated from the processes that characterize biochemical consumption in the sediments and the water column. Under these conditions, the parameters related to biochemical consumption in the sediments can be used to compute the expected DO demanded of the sediments in field conditions. Sediment samples from a lagoon near the Universidad de Chile campus in Santiago, the capital city of Chile, were used to illustrate the application of the proposed method. In addition, dimensionless numbers were used to define the method's validity and limitations. **DOI: 10.1061/(ASCE)EE.1943-7870.0000926.**

Author keywords: Benthic chamber; Sediment oxygen demand; Turbulent diffusion; Experimental methods.

Introduction

One of the most important variables in aquatic ecosystems is dissolved oxygen (DO) concentration, which defines the viability threshold for life and the dominant chemical speciation of different elements (Wetzel 2001). The DO concentration in a specified volume depends on the DO sources and sinks in the control volume (Odum 1956; Ryther 1956; Herzfeld et al. 2001) and on the DO fluxes across boundaries. These DO exchanges with the surrounding ambient include advective and diffusive fluxes across open boundaries and the diffusive fluxes across the air-water (Guatieri and Gualtieri 2008) and water-sediment interfaces (WSI) (Jørgensen and Des Marais 1990; Dade 1993). The DO flux across the WSI, hereafter referred to as $J(\mathrm{gO_2m^{-2}\,d^{-1}})$, depends on the diffusive transport on both sides of the interface (Jørgensen and Des Marais 1990; Mackenthun and Stefan 1998; O'Connor and Hondzo 2008) and on the rate of DO production and consumption in the sediment (Bouldin 1968; Jørgensen et al. 1983; Kühl and Jørgensen 1992).

Multiple techniques can be used to measure DO flux across the WSI, including DO microprofiles and benthic chambers. DO microprofiles are effective for measuring J in situ and in the laboratory. Since early applications of this technique (Revsbech et al. 1980a, b), several studies have shown that microprofiles provide detailed information that can be used to quantify mass exchanges across the WSI and biochemical processes in sediments (e.g., Jørgensen and Revsbech 1985; Jørgensen and Gundersen 1990; de la Fuente 2014). Based on microprofile measurements, J can be determined in at least five different forms (see Bryant et al. 2010 for a review). However, microprofiles are expensive and fragile instruments that require sophisticated equipment for collecting precise measurements (with a resolution of micrometers) (Kemp et al. 1993; Berg et al. 1998; de la Fuente 2014). Also, their measurements are representative of a very small area of the sediments near the tip of the microelectrode, and it is not clear how to integrate them into larger areas (Kemp et al. 1993; Viollier et al. 2003; Roy et al. 2005). In contrast, benthic chambers are inexpensive, robust, and easily implemented in laboratory and field conditions (Hall et al. 1989; Herzfeld et al. 2001; Viollier et al. 2003; Arega and Lee 2005). Benthic chambers isolate a volume of water from its surrounding fluid. The DO depletion rates within them are used to compute J (e.g., Sommer et al. 2008; Jahnke et al. 2008; Gao et al. 2012).

The problem with benthic chambers is that the computed J is only valid for turbulent conditions inside the chamber (Mackenthun and Stefan 1998; Viollier et al. 2003). To address this limitation, Tengberg et al. (2004), Arega and Lee (2005), and Ferrón et al. (2008), among others, studied the hydrodynamic conditions inside benthic chambers for obtaining curves that relate operational conditions (e.g., stirring rate, exchanged-flow rate) to the diffusional mass transfer coefficient, k_t, which is the turbulent parameter that drives (e.g., Dade et al. 2001). The rate at which gypsum plates in a benthic chamber are dissolved can be used to estimate k_t inside them (Santschi et al. 1983; Tengberg et al. 2004). As Viollier et al. (2003) pointed out, one of the four basic assumptions required for computing J in a benthic chamber is that "the hydrodynamic regime inside the chamber does not alter solute exchange across the sediment-water interface as compared to natural conditions." However, the authors also stated that this assumption is not always true,

[1]Departamento de Ingeniería Civil, Universidad de Chile, Santiago 8370449, Chile. E-mail: aldelafu@ing.uchile.cl

Note. This manuscript was submitted on January 21, 2014; approved on November 18, 2014; published online on December 24, 2014. Discussion period open until May 24, 2015; separate discussions must be submitted for individual papers. This paper is part of the ***Journal of Environmental Engineering***, © ASCE, ISSN 0733-9372/04014098(11)/$25.00.

which must be kept in mind during data analysis and interpretation of results.

The purpose of this article is to present a method for analyzing the DO time series inside a benthic chamber which isolates the influence of turbulent transport in the chamber from the rest of the processes. This method can be used to understand the DO consumption rate in sediments without the influence of flow conditions. To illustrate the method, four laboratory experiments were conducted in a benthic chamber with sediment samples collected from the lagoon of a park near the Universidad de Chile campus in Santiago. In addition, DO consumption in the sediments was characterized with DO microprofiles and dimensionless numbers were used to define the proposed method's application range.

The article is organized as follows. First, the theoretical background, experimental apparatus, and proposed method for analyzing DO time series in a benthic chamber are presented. Next, the proposed method and a sensitivity analysis are applied to four experiments. Lastly, results are discussed.

Materials and Methods

DO Flux across the WSI

The proposed methodology uses the early conceptual model of Nakamura and Stefan (1994) to compute the downward flux of DO across the WSI, J $\mathrm{gO_2\,m^{-2}\,d^{-1}}$. This equation can be written as

$$J = k_t\left(C - \frac{J^2}{S}\right) \tag{1}$$

or as

$$J = \frac{S}{2k_t}\left(-1 + \sqrt{1 + \frac{4k_t^2}{S}C}\right) \tag{2}$$

where C = DO concentration in the water column outside the benthic boundary layer; and $k_t(\mathrm{md^{-1}})$ = mass transfer velocity or diffusional mass transfer coefficient (Dade 1993; Steinberger and Hondzo 1999; Hondzo et al. 2005).

In addition, $S = 2\phi R_{O_2} D_s(\mathrm{gO_2\,m^{-1}\,d^{-2}})$ is a coefficient that quantifies all of the processes that occur in the sediments, where R_{O_2} is the bulk rate of volumetric DO consumption $\mathrm{gO_2\,m^{-3}\,d^{-1}}$, ϕ is the upper sediment porosity, which can be assumed to be 0.95 (Bryant et al. 2010), and $D_s(\mathrm{m^2\,d^{-1}})$ is the DO diffusion coefficient, which also depends on porosity (Rasmussen and Jørgensen 1992; Bryant et al. 2010). Here, $D_s = D\phi$ with D the molecular diffusion that depends on water temperature. Use of a homogeneous R_{O_2} is supported by the observations of Kühl and Jørgensen (1992) and Rasmussen and Jørgensen (1992). More discussion on this assumption is given in later sections of this article.

The solution of Eq. (2) is asymptotic to $J_{\mathrm{lim}} = \sqrt{SC}$ when $k_t \to \infty$. This situation occurs when the biochemical consumption rate limits the J value. In contrast, when turbulent diffusion across the WSI is the limiting factor (equivalent to large S), the J value is asymptotic to $k_t C$. Fig. 1(a) shows the curve JJ_{lim}^{-1} as function of $k_t C J_{\mathrm{lim}}^{-1}$. Both asymptotic limits are shown in the figure, which depicts the relationship between J and k_t . Furthermore, Fig. 1(b) shows the Jk_tS^{-1} values as a function of $Ck_t^2S^{-1}$, where the limit $J \approx k_t C$ is represented by the dashed line. This figure represents the relationship between J and C.

An alternative mathematical model for computing J as a function of C is (Jørgensen and Bendoricchi 2001; Hipsey et al. 2014)

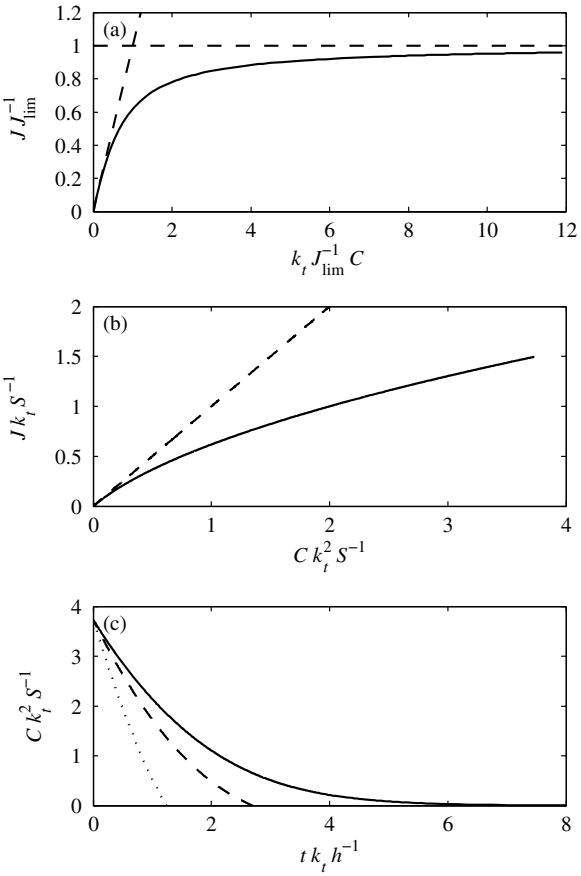

Fig. 1. (a) Dimensionless DO flux across the WSI as a function of dimensionless transfer velocity [dashed lines = asymptotic values of J depending on the region in which the flux was limited by turbulent transport (diagonal) or the rate of biochemical consumption in the sediments (horizontal)]; (b) relationship between the dimensionless DO flux across the WSI and the DO concentration (dashed line = asymptotic values of J in which the flux was limited by turbulent transport); (c) time series of the dimensionless DO concentration in the benthic chamber computed with Eq. (6) [solid line = $(2k_t r_w/S) = 0$; dashed line = $(2k_t r_w/S) = 0.5$; dotted line = $(2k_t r_w/S) = 2$]

$$J = k_s \frac{C}{(k_{O_2} + C)} \tag{3}$$

where $k_s(\mathrm{grO_2\,m^{-2}\,d^{-1}})$ = specific rate of DO consumption in the sediments [determined in a benthic chamber (Jørgensen and Bendoricchi 2001)] and $k_{O_2}(\mathrm{grO_2\,m^{-3}})$ the half-saturation constant for the Michaelis-Menten limitation of J in terms of C.

However, J as computed with Eq. (3) does not include the role of turbulence inside the benthic chamber, so it is not useful for the purposes of this article. A similar situation can be found with another mathematical representation of J (Jørgensen and Bendoricchi 2001; Cole and Buchak 1995) that also neglects the effect of k_t on J.

DO Mass Conservation in Benthic Chambers

If the changes in C inside a benthic chamber occur over a longer period than the duration of diffusion in the sediments, the accumulation/depletion rate of DO in the sediments can be neglected. In this case, Eq. (2) is assumed to represent the flux across

the WSI for unsteady conditions. With this, the biochemical oxygen demand (BOD) in the water column is included and the mass conservation of DO in a benthic chamber is written as

$$V\frac{dC}{dt} = -AJ - Vr_w = -A\frac{S}{2k_t}\left(\sqrt{1+\frac{4k_t^2}{S}C}-1\right) - Vr_w \quad (4)$$

where V = volume of the chamber; A = area exposed to the sediments; and r_w ($gO_2\ m^{-3}\ d^{-1}$) = rate of DO consumption in the water column due to BOD.

BOD degradation is usually represented with a first-order kinetic reaction such that (Jørgensen and Bendoricchi 2001)

$$-r_w = \frac{d\text{BOD}}{dt} = -\alpha\text{BOD} \quad (5)$$

where α = first-order rate coefficient of BOD degradation. The coefficient α takes values in the range of $\alpha = 0.05$–$0.15\ d^{-1}$ for rivers and drinking water (Jørgensen and Bendoricchi 2001). With a constant value of α, the solution of Eq. (5) provides that $r_w(t) = \alpha\text{BOD}_o \exp(-\alpha t)$, where BOD_o is the initial condition of the problem. However, in a timescale of one experiment (1 day), r_w varies only 5–15%, so it can be assumed constant. This assumption simplifies the integration of Eq. (4) and reduces from two (α and BOD_o) to one (r_w) the number of parameters required for characterizing BOD. With this simplification (r_w = constant), the analytic solution of Eq. (4) is written as

$$\begin{aligned}-k_t\frac{t}{h} = &\left(1-\frac{2k_t r_w}{S}\right)\ln\left(\sqrt{1+\frac{4k_t^2}{S}C}+\frac{2k_t r_w}{S}-1\right)+\sqrt{1+\frac{4k_t^2}{S}C}\\ &-\left(1-\frac{2k_t r_w}{S}\right)\ln\left(\sqrt{1+\frac{4k_t^2}{S}C_o}+\frac{2k_t r_w}{S}-1\right)\\ &-\sqrt{1+\frac{4k_t^2}{S}C_o}\end{aligned} \quad (6)$$

where C_o = initial concentration; and $h = V/A$.

The time series of C, which is described by Eq. (6), is shown in Fig. 1(c).

Finally, when C approaches zero, $J \approx k_t C$ and Eq. (4) becomes independent of the parameter S and is written as

$$h\frac{dC}{dt} = -k_t C - hr_w \quad (7)$$

Eq. (7) shows that for small DO concentrations, the linear rate of DO depletion inside the benthic chamber is given by hr_w whereas the curvature of this decay is controlled by k_t. The analytic solution of Eq. (7) is

$$C(t) = \left(C_o + \frac{hr_w}{k_t}\right)\exp\left(-k_t\frac{t}{h}\right) - \frac{hr_w}{k_t} \quad (8)$$

where C_o = initial condition.

Eq. (8) is used to fit the value of the parameters k_t and r_w.

Experimental Facility

Experiments were conducted in a benthic chamber in which a volume of water was isolated from the atmosphere and from lateral DO fluxes to obtain a time series of DO exchange across the WSI and BOD (Hall et al. 1989; Herzfeld et al. 2001; Arega and Lee 2005). The DO mass balance in the benthic chambers is described by Eq. (4). Fig. 2(a) shows the experimental setup.

The benthic chamber consisted of a closed acrylic cylinder of 12 cm height and 4 cm inner diameter. Both top and base covers were removable and were screwed to the cylinder. DO and water temperature were measured with the CellOx 325 sensor (WTW, Weilheim, Germany), which was mounted in a tube of 1.5 cm inner diameter fixed to the top cover. Because the solutes of the benthic chamber must be homogeneously mixed to use Eq. (4), the water was stirred with a standard magnetic stirrer that rotated over a perforated plate located approximately 3 cm above the WSI. The plate was perforated with 21 holes of inner diameter 5 mm arranged as shown in Fig. 2(b). Effective mixing across the perforated plate was tested by placing inked water below the plate, and well-mixed conditions were observed a few seconds after the magnetic stirrer was switched on. Finally, the sediment sample was placed in a cylindrical compartment of 3.6 cm inner diameter located on the bottom of the chamber.

The total volume of the benthic chamber was $V = 132$ ml with a height of $h = VA^{-1} = 13$ cm, indicating that DO concentrations were expected to change by $5\ gO_2\ m^{-3}$ over 12 h. This result was based on a characteristic value of $\tilde{J} = 1.3\ gO_2\ m^{-2}\ d^{-1}$, which was obtained from the results of Arega and Lee (2005), Gin and Gopalakrishnan (2010), and Inoue and Nakamura (2011).

Justification is required for the use of the steady-state solution of Eq. (2) to compute J in a problem where C changes in time. Particularly, Eq. (2) can be used if the timescale in which C varies is within the timescale in which diffusion in the sediments occurs. Then a permanent solution is rapidly reached in the sediment. The timescale of changing C inside the benthic chamber was estimated based on Eq. (4) and $r_w = 0$:

$$T_c = \frac{h\Delta C}{\tilde{J}} \quad (9)$$

where ΔC = characteristic concentration fluctuation equal to the accuracy of the instrument ($\Delta C = 0.1\ gO_2\ m^{-3}$).

In contrast, the diffusion timescale in the sediments was estimated as

$$T_d = \frac{(\Delta\delta)^2}{\phi D_s} \quad (10)$$

where $\Delta\delta$ = changes in the penetration depth of oxygen into the sediments due to changes in DO concentration in the benthic chamber.

The penetration depth is written as (Bouldin 1968; Kühl and Jørgensen 1992; Rasmussen and Jørgensen 1992)

$$\delta = \frac{2\phi D_s\tilde{J}}{\tilde{S}} \approx 1.7\ \text{mm} \quad (11)$$

where $\tilde{S} = 0.38\ (gO_2\ m^{-1}\ d^{-2})$, a characteristic value of S that was estimated with $\tilde{J} = 1.3\ (gO_2\ m^{-2}\ d^{-1}) = \sqrt{\tilde{S}\tilde{C}}$ and $\tilde{C} = 5(gO_2\ m^{-3})$.

Finally $\Delta\delta$ is written as

$$\Delta\delta = \frac{2\phi D_s}{\tilde{S}}\left(\tilde{J} - \sqrt{\tilde{S}(\tilde{C}-\Delta C)}\right) \approx 0.02\ \text{mm} \quad (12)$$

In this way, $T_d \approx 0.15$ s and $T_c \approx 18$ min. As a consequence, the timescale at which C varies inside the chamber is much greater than the timescale at which diffusion from the sediments occurs, justifying the use of Eq. (2) to compute J.

Experimental Procedure

Sediment samples were collected from the artificial lagoon of O'Higgins Park near the University campus in Santiago, Chile.

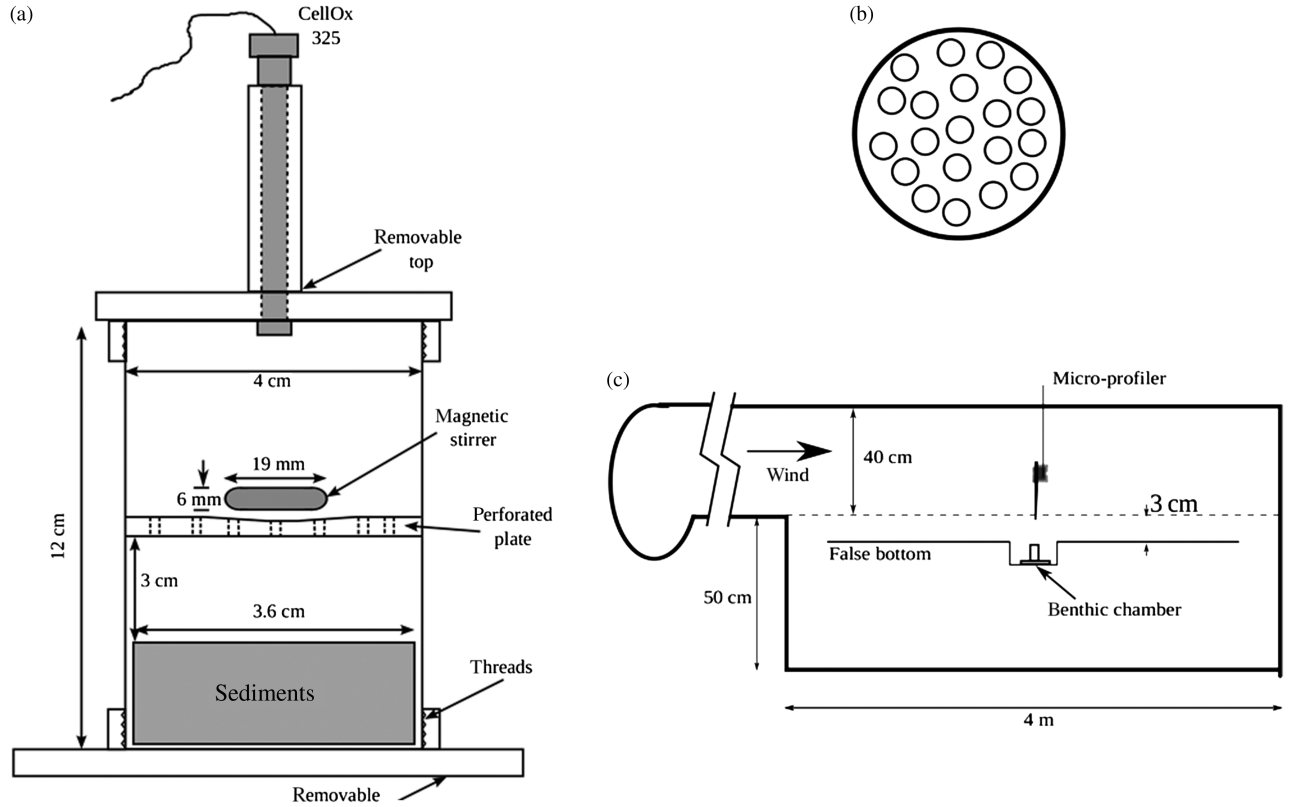

Fig. 2. Experimental setup

Before each experiment, the sediment cores were installed in the benthic chamber and allowed to equilibrate for 3 h. During the equilibration period, the magnetic stirrer was on and the top cover was unmounted.

The experiment began when the DO sensor was placed and sealed with silicone. The DO and water temperature time series from inside the benthic chamber was recorded with a CellOx325 sensor each minute. Resolution of the sensor was 0.01 $gO_2\,m^{-3}$ and 0.1°C, and the accuracy was 0.05% and 0.1°C for DO and temperature, respectively. The 95% response time of the sensor was 16 s, and the self-consumption rate of DO was 0.08 $\mu g\,h^{-1}(mgl^{-1})^{-1}$, which was neglected because it was equivalent to $J = 0.01(gO_2\,m^{-2}\,d^{-1})$. The CellOx325 sensor was calibrated according to the procedure described in the user manual. The first three hours of measurements were not included in the analysis.

Four experiments were conducted to illustrate the application of the method. Experiments 1 and 2 were conducted with drinking water and with angular velocities of the magnetic stirrer of 3 and 5.2 Hz, respectively. Experiments 3 and 4 used distilled water and angular velocities of 3 and 5.2 Hz, respectively. The experimental conditions of each experiment are summarized in Table 1, and the measured time series of DO and temperature are shown in Fig. 3. The angular velocity of the magnetic stirrer was measured with a camera recording at 60 fps. Unfortunately, it was not possible to use other angular velocities to obtain a detailed curve of k_t versus ω.

Microprofiles

To test the accuracy of the method, DO microprofiles were measured with one OX25 Unisense microelectrode and the corresponding Unisense Microsensor Multimeter data amplifier and Unisense Sensor Trace PRO acquisition software (Unisense, Aarhus, Denmark). The calibration of the microelectrode was conducted as described in the user manual. Microprofiles were measured with the sediment sample inside the benthic chamber without the top cover and the magnetic stirrer. Turbulence in the water column was produced with the wind tunnel shown in Fig. 2(c) (Ordoñez et al. 2013). The wind tunnel had on its down-wind end a 4-m long, 0.5-m wide, and 0.5-m deep tank containing a false bottom 3 cm below the bottom of the wind tunnel. In the middle of the false bottom there was a 0.15-m long compartment where the benthic chamber was placed [Fig. 2(c)]. The microelectrode was mounted on a gauge set on a platform over the wind tunnel; the elevation of the gauge was automatically manipulated with an electronic motor. Microprofiles were measured with drinking and distilled water in

Table 1. Summary of Experimental Conditions

Run	Water	Duration (d)	ω (Hz)	DO ($gO_2\,m^{-3}$)	T (°C)	$\nu \times 10^6$ ($m^2\,s^{-1}$)	Sc	n
1	Drinking	1.34	3.0	0–7.19	23.4 ± 1.5	0.932	433	1,924
2	Drinking	0.84	5.2	0–6.86	23.9 ± 1.2	0.922	424	1,212
3	Distilled	0.64	3.0	0–5.29	24.2 ± 1.0	0.915	416	928
4	Distilled	0.84	5.2	0–6.95	24.3 ± 1.4	0.913	415	1,212

Note: Duration indicates length of the time series used for the analysis; ω = angular velocity of the magnetic stirrer; DO = range of variation of DO concentration; T = average temperature ± standard deviation; ν = water viscosity; Sc = Schmidt number; and n = length of time series.

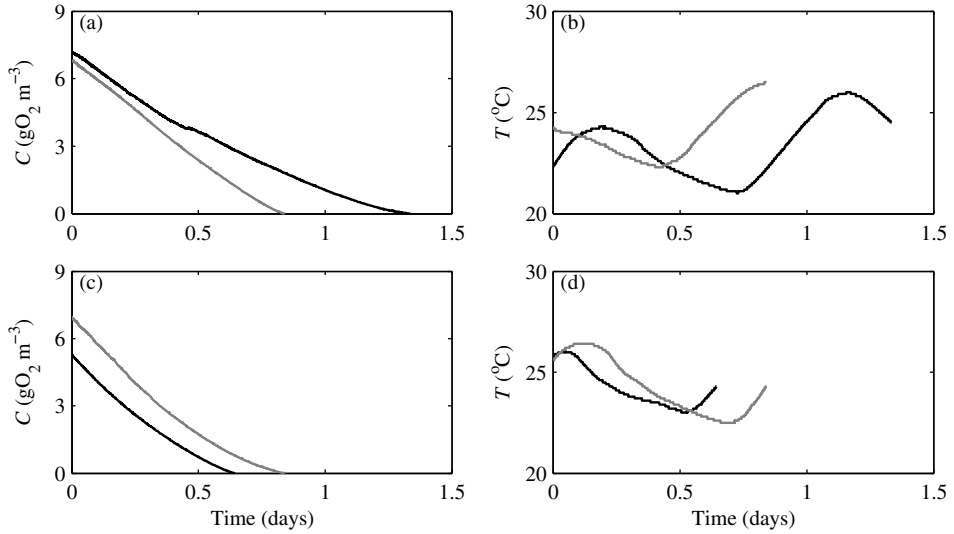

Fig. 3. Measured time series of DO and water temperature for experiments with (a and b) drinking water; (c and d) distilled water, black line = experiment with $\omega = 3$ Hz; gray line = experiment with $\omega = 5.2$ Hz

the benthic chamber, and two replicates were obtained for each type of water used (dr1 and dr2 for drinking water and ds1 and ds2 for distilled water)

Vertical spacing for the microprofiler was set to 160 μm in the sediments and 200 μm in the water column. Each microprofile was conducted based on 90-s cycles, recorded at 1 Hz, in which the first 30 s were spent moving the microelectrode between two consecutive elevations and acclimating the sensor to the new conditions; the last 60 s corresponded to measurements that were averaged for obtaining the final DO concentration.

For each microprofile, three characteristic values of S were obtained. First, to use a homogeneous $S = 2\phi R_{O_2} D_s$ in the sediments means that DO concentration follows a quadratic equation, with the depth, z, being the coefficient associated with z^2 equal to $S/(2\phi D_s)^2$. Consequently, the first characteristic S (called S_I) was obtained by fitting a quadratic equation to a microprofile of the DO concentrations in the sediments. Furthermore, the vertical DO gradient has a maximum absolute value at the WSI and linearly decreases with depth at a slope equal to $S/(2\phi D_s)^2$. The vertical gradient of DO at the ith elevation in the profile was obtained as the slope of the linear regression computed with the points $i-2$, $i-1$, i, $i+1$, and $i+2$. The second characteristic value of S (called S_{II}) was then computed as the slope of linear fit of these DO vertical gradients with respect to the elevation. Finally, J can also be computed as $J = \sqrt{SC_s}$, where C_s denotes the concentration at the WSI (Bouldin 1968). On this basis, a third characteristic value of S was computed as $S_{\mathrm{III}} = J^2/C_s$, where J is the diffusive flux at the WSI and C_s is the observed DO concentration at the WSI.

Fitting Algorithm and Confidence Interval

The fitting algorithm used to obtain the value of the coefficients S, k_t, and r_w of Eqs. (4) and (7) was based on nonlinear parameter fitting (Seber and Wild 2003), accomplished using the standard Gauss-Newton iterative method in *MATLAB*. However, this nonlinear fitting problem can also be solved with the *Solver* function in MS-Excel or with more sophisticated functions in *MATLAB* like *fit* or *lsqcurvefit*.

The Gauss-Newton iterative method considers a data set with n pairs of dependent (Y_i) and independent (X_i) variables. In addition, a continuum function $[F(\alpha_j, X)]$ was fitted to the observed variables to obtain the parameters of the problem α_j, α_j being equal to S, k_t, or r_w. This method minimizes the least-squares error. The iterative procedure also considers that the values of the parameters α_j are known for a particular iteration. These values are corrected and used in the following iteration:

$$\Delta\alpha_j = \frac{\sum_{i=1}^{n} \frac{\partial F_i}{\partial \alpha_j}(Y_i - F_i)}{\sum_{i=1}^{n} (\frac{\partial F_i}{\partial \alpha_j})^2} \tag{13}$$

where $F_i = F(\alpha_j, X_i)$.

The gradients of F are numerically estimated as $\partial F_i/\partial \alpha_j = [F(\alpha_j + \delta, X_i) - F(\alpha_j, X_i)]/\delta$, and $\delta = 1 \times 10^{-10}$. The procedure ends when the following result occurs: $\max[\mathrm{abs}(\Delta\alpha_j)/\alpha_j] < 1 \times 10^{-4}$. Each parameter is given an initial value of 1 prior to the iteration.

A confidence interval of 95% for each estimated parameter was used to estimate error. These confidence intervals were computed using the nonlinear least-squares estimation described in Seber and Wild (2003). The upper and lower confidence limits of α_j were defined by the roots, $\widehat{\alpha}_j$, of the following second-degree polynomial equation:

$$(\widehat{\alpha}_j - \alpha_j)^2 \sum_{i=1}^{n} \left(\frac{\partial F_i}{\partial \alpha_j}\right)^2 = \frac{p}{n-p} f_{p,n-p}^{0.95} \sum_{i=1}^{n} (Y_i - F_i)^2 \tag{14}$$

where $f_{p,n-p}^{0.95}$ = inverse of the 95% accumulative probability distribution function, F, with two degrees of freedom, p, and $n-p$, where p = the number of fitting parameters.

The roots of Eq. (14) are symmetric with respect to the fitted α_j. Thus, the confidence interval can be written as

$$\widehat{\alpha}_j = \alpha_j \pm \sqrt{\frac{\frac{p}{n-p} f_{p,n-p}^{0.95} \sum_{i=1}^{n} (Y_i - F_i)^2}{\sum_{i=1}^{n} (\frac{\partial F_i}{\alpha_j})^2}} \tag{15}$$

Methodology for Fitting of S

A two-step fitting methodology was used. First, the values of two parameters, r_w and k_t, must be known before obtaining the value of S. For each experiment, these values were obtained by fitting

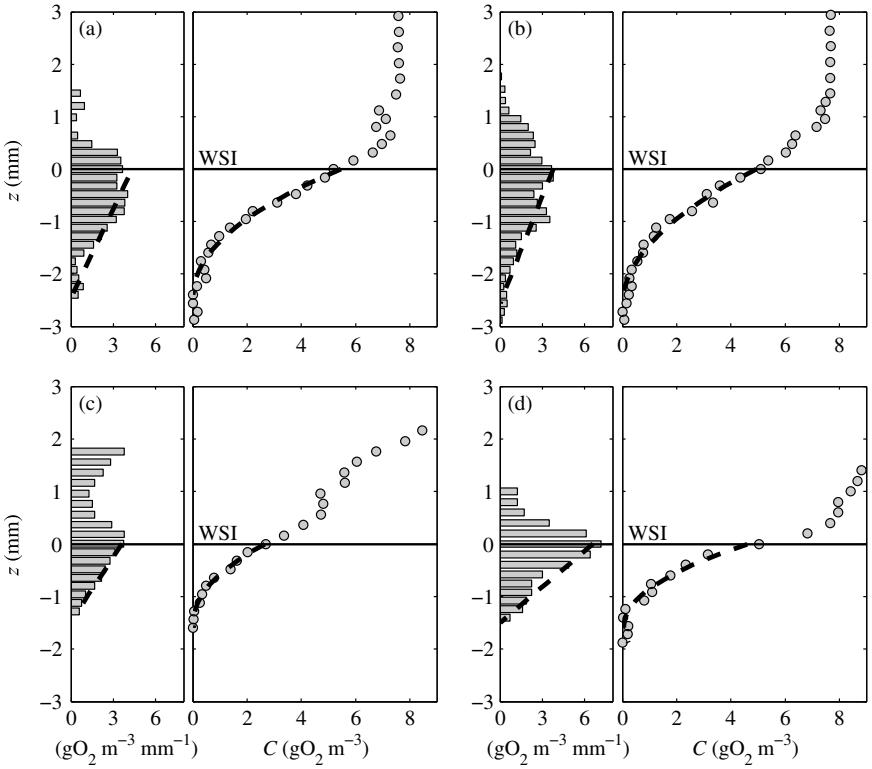

Fig. 4. DO microprofiles (gray circles) and vertical gradient of DO (horizontal bars): (a and b) dr1 and dr2 with drinking water; (c and d) ds1 and ds2 with distilled water; dashed lines = fitted curves for characteristic values obtained for the coefficient S

Eq. (8) with the data set of small DO concentrations, defined as $C \leq 0.3$ $gO_2\,m^{-3}$. Based on the notation used in Eqs. (13)–(15), C was used as the dependent variable (Y), the time t was used as the independent variable (X), and there were three parameters to fit: $\alpha_j = k_t$, r_w, and C_0 [$p = 3$; see Eq. (14)], where C_0 was a auxiliary parameter not relevant in the analysis.

With these fitted values of k_t and r_w, two alternatives for analyzing the DO time series were tested. The first alternative required a data set of $h\partial C/\partial t$ versus C for a fixed flow velocity inside the benthic chamber. Based on the notation used in Eqs. (13)–(15), $h\partial C/\partial t$ was used as the dependent variable (Y), C was used as the independent variable (X), and one parameter was fit [$\alpha_j = S$; $p = 2$; see Eq. (14)]. The rate of DO depletion in the benthic chamber ($\partial C/\partial t$) was computed as the slope of the linear fit of 30 min of measurements, and C was computed as the average value of those measurements. The second alternative to obtain the value of S used the DO time series inside the benthic chamber. These data were fit with Eq. (5) to obtain $\alpha_j = S$ and C_o [$p = 2$; see Eq. (14)]. Again, C_o was an auxiliary parameter not relevant in the analysis. Because it was not possible to obtain an algebraic expression for $C(t)$, it was more efficient to fit t as a function of C. In this case, the independent variable (X) was C and the dependent variable (Y) was t.

Results

DO Microprofiles

Fig. 4 shows the four measured DO micro-profiles (gray circles) and the corresponding vertical gradient of DO (horizontal bars) having positive values because the DO flux is against the z-axis. The dashed lines show the fitted curve for measuring S based on the quadratic fitting of DO concentration in the sediments (S_I) and the linear fit of the DO diffusive fluxes (S_{II}). Table 2 summarizes the results of Fig. 4, where it is observed that S_I, S_{II}, and S_{III} have similar values with a standard deviation of less than 20% with respect to the average. Thus, it is argued that the microprofile process was correct and that the average value of S characterized the biochemical processes in the sediment sample. One important observation was that the value of S computed for distilled water was approximately twice as large as the value obtained for drinking water (0.260 and 0.116 $gO_2\,m^{-1}\,d^{-2}$, respectively). This influence of the water used in the benthic chamber was also noticed in the benthic chamber measurements; however, studying this relationship was not an objective of this study.

Fitting of S

Table 3 shows, for each experiment, the fitted values of k_t and r_w. Fig. 5 compares the observed DO concentrations and the fitted Eq. (7). The average k_t for $\omega = 3$ and 5.2 Hz were 0.71 and 1.01 md^{-1}, respectively. Unfortunately, operational restrictions with the magnetic stirrer prevented measuring other values of ω. The determination coefficient in all experiments was close to 1, and the confidence interval of r_w and k_t was also small.

Table 2. Summary of Microprofile Results

		$S\,(gO_2\,m^{-1}\,d^{-2})$			
Run	Water	S_I	S_{II}	S_{III}	Average ± standard deviation
dr1	Drinking	0.144	0.134	0.098	0.116 ± 0.019
dr2		0.109	0.112	0.100	
ds1	Distilled	0.178	0.188	0.193	0.260 ± 0.088
ds2		0.280	0.335	0.388	

Table 3. Summary of Results from Fitting of r_w, k_t, and S

Run	ω (Hz)	k_t (md^{-1})	r_w ($gO_2\,m^{-3}\,d^{-1}$)	S_1 ($gO_2\,m^{-1}\,d^{-2}$)	S_2 ($gO_2\,m^{-1}\,d^{-2}$)	S ($gO_2\,m^{-1}\,d^{-2}$)
1	3.0	0.756 ± 0.052	1.376 ± 0.053	0.147 ± 0.018	0.159 ± 0.002	0.156 ± 0.023
		r^2:0.99, n:199		r^2:0.80, n:62	r^2:0.99, n:1,864	
2	5.2	1.157 ± 0.148	3.538 ± 0.156	0.133 ± 0.022	0.187 ± 0.003	
		r^2:0.99, n:0.91		r^2:0.20, n:40	r^2:0.99, n:1,212	
3	3.0	0.656 ± 0.148	3.775 ± 0.164	0.321 ± 0.017	0.312 ± 0.001	0.377 ± 0.077
		r^2:0.99, n:0.95		r^2:0.99, n:30	r^2:1.00, n:928	
4	5.2	0.861 ± 0.104	2.282 ± 0.107	0.398 ± 0.058	0.476 ± 0.002	
		r^2:0.99, n:136		r^2:0.85, n:40	r^2:0.99, n:1,212	

Note: ω = angular velocity of magnetic stirrer; n = number of points in the data set; r^2 = coefficient of determination. S_1 was obtained with alternative 1; S_2, with alternative 2.

Using the fitted parameters k_t and r_w, the coefficient S was computed following alternatives 1 and 2—S_1 and S_2 in Table 3, respectively. The average fitted S for distilled water was $0.377(gO_2\ m^{-1}\,d^{-2})$, which is 2.4 times larger than the fitted value for drinking water, $S = 0.156(gO_2\,m^{-1}\,d^{-2})$. Fig. 6 shows that this result is congruent with microprofile observation; however, the ration between observed S values in the benthic chamber and those observed in the micro-profiles was 1.41 (1.34 for drinking water and 1.46 for distilled water). This difference can be attributed to the fact that microprofiles represent localized processes whereas a benthic chamber represents the surface integrated value of S. Further arguments to support this hypothesis are given in the discussion.

The results shown in Fig. 7 indicate that the fitting technique and the theoretical background represent the measurements sufficiently to explain the long-term evolution of DO inside the benthic chamber. The figure compares measurements and fitted curves for obtaining S coefficients following alternative 1 [Figs. 7(a, c, e, g)] and alternative 2 [Figs. 7(b, d, f, h)]. The fitted curves agreed well with the measurements over the entire range of observations. This agreement was especially prevalent in experiments 1, 3, and 4, where the observations followed the same curvature predicted by Eqs. (4) and (6). The determination coefficients r^2 in alternative 2, were very close to 1 in all experiments (Table 4 and the numbers in bracket in Fig. 6); however, the values of r^2 in alternative 1 were smaller because alternative 1 required localized observations of only 30 min whereas alternative 2 integrated these fluxes over a long period of time. As a consequence, alternative 2 smoothed the solution so its obtained determination coefficients were much larger than the corresponding value obtained by alternative 1.

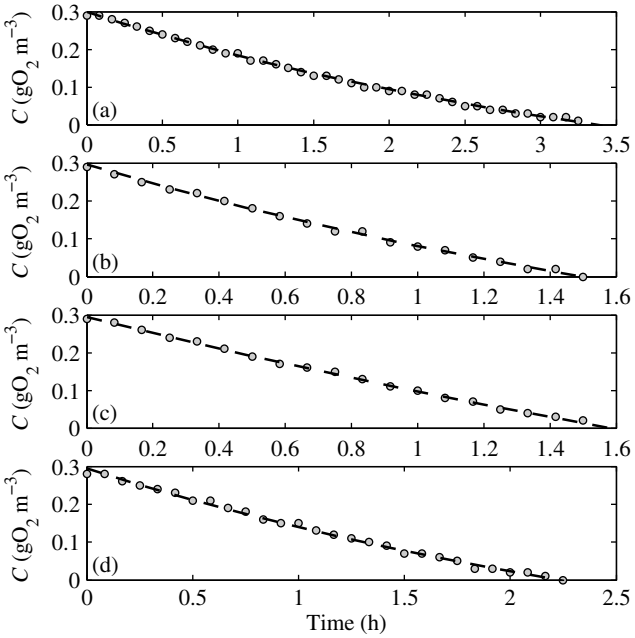

Fig. 5. Time series of DO concentration for $C < 0.1\ gO_2\,m^{-3}$ (dashed lines = fitted curve for obtaining coefficients k_t and r_w): (a) experiment 1; (b) experiment 2; (c) experiment 3; (d) experiment 4

The two-step fitting methodology was required because the dimensionless number $k_tC/\sqrt{SC}$ was larger than 2 for most of the measured C, which means that J was more dependent on S than k_t [Fig. 1(a)]. Thus, if k_t, r_w, and S were fitted at once with the entire data set, the fitted coefficient k_t would be unrealistically large (on the order of 1,000 md^{-1}) with an even larger confidence interval.

Sensitivity Analysis

A sensitivity analysis was required to quantify the influence of coefficients k_t and r_w on coefficient S in order to recompute S using the fitted k_t and r_w coefficients $\pm 20\%$.

Fig. 8 summarizes the results of the sensitivity analysis. First, increasing or decreasing r_w or k_t reduces or increases the fitted value of S. Thus, it is observed that increasing the transfer velocity by 20% produces, on average, a reduction in S smaller than 10%. On the other hand, reducing the value of k_t by 20% causes S to increase by approximately 13%. However, ΔS in the sensitivity analysis for r_w has the same order of magnitude as the corresponding Δr_w, which suggests that the uncertainty in estimating r_w is directly transmitted to estimating S.

Moreover, k_t and r_w were estimated with Eq. (8), which required $J \approx k_tC$. This simplification is valid for small values of $k_tC/\sqrt{SC}$ [Fig. 1(a)] and underestimates k_t. Using the average S and $C \leq 0.3(gO_2\,m^{-3})$, the average $k_tC/\sqrt{SC}$ was computed and the average percentage of error associated with the assumption $J = k_tC$ was estimated as

$$\Delta J = 100\text{avg}\left(\frac{(k_tC - J)}{J}\right) \tag{16}$$

In Eq. (16) J was computed with Eq. (2), so the error in k_t due to the assumption $J \approx k_tC$ (called Δk_t^*) was estimated from

$$\Delta J = \frac{\partial J}{\partial k_t}\Delta k_t^* \tag{17}$$

Table 4 summarizes the average $k_tC/\sqrt{SC}$, ΔJ, and Δk_t^*. As shown, the approximation $J \approx k_tC$ has a 15% error for experiments in distilled water and a 32% error for those in drinking water. This difference is explained by the value S in distilled water, which was larger than that in drinking water. The errors in the estimation of

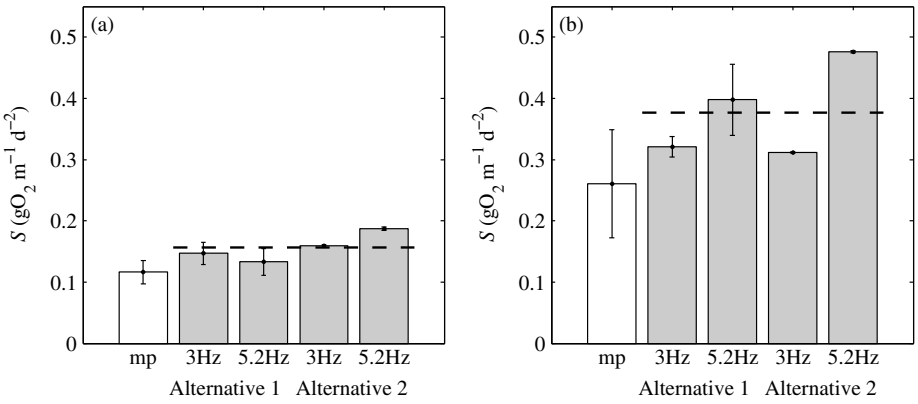

Fig. 6. Results from fitting coefficient S: (a) experiments 1 and 2; (b) experiments 3 and 4; white bars = microprofile measurements; gray bars = experiment with angular frequencies; processing alternatives are shown on the horizontal axis; dashed line = average of coefficient S

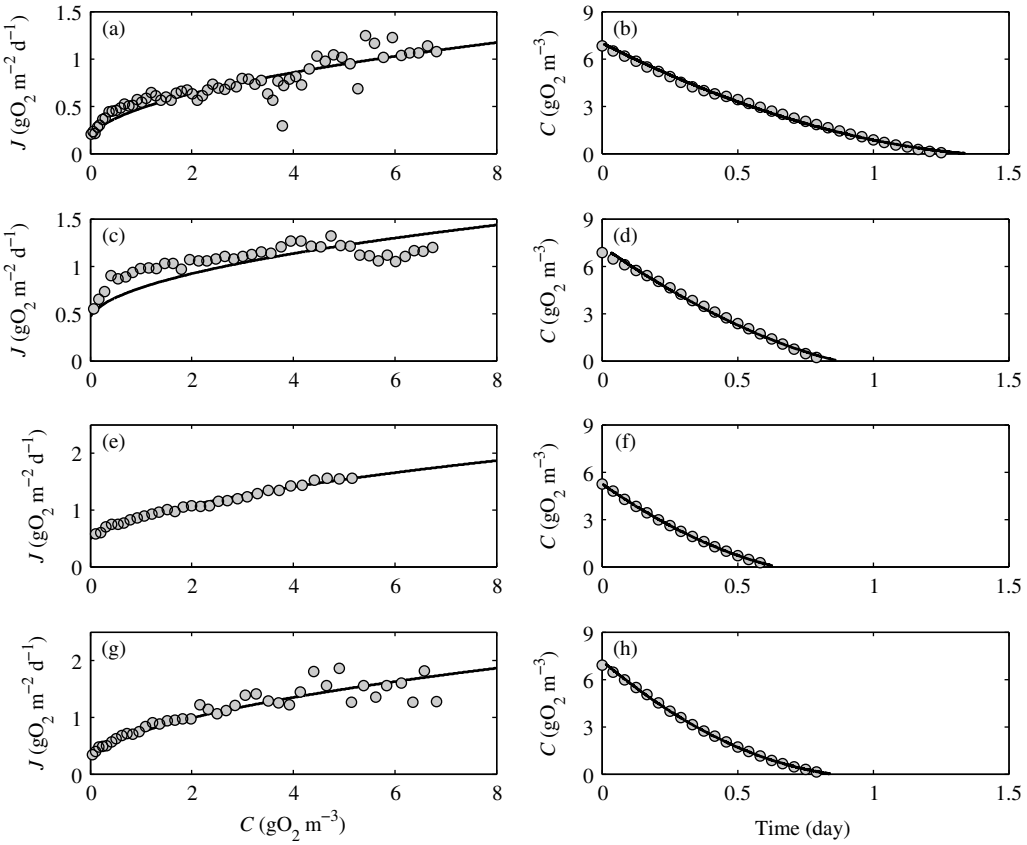

Fig. 7. Results from fitting coefficient S: comparison of measured (circles) and fitted (line) values as a function of DO concentration in the benthic chamber for each experiment listed in Table 1; (a, c, e, and g) fitting of coefficient S following alternative 1; (b, d, f, and h) fitting of coefficient S following alternative 2; (a and b) experiment 1; (c and d) experiment 2; (e and f) experiment 3; (g and h) experiment 4

Table 4. Estimation of the Error in the Estimation of k_t with Eq. (8)

Run	$\text{avg}\left(\frac{k_t C}{\sqrt{SC}}\right)$	ΔJ (%)	Δk_t^* (%)
1	0.67	24.5	28
2	1.10	40.0	111
3	0.48	16.1	12
4	0.47	15.8	11

Note: The coefficient S is the average value of the table. ΔJ was defined in Eq. (16); Δk_t^*, in Eq. (17).

J produced errors in the estimation of k_t estimated to be 11% in distilled water and 28% in experiment 1. The error in the estimation of k_t in experiment 2 was very large, and in such cases repeating the measurements is recommended. Finally, given that Eq. (9) underestimates the value of k_t, the sensitivity analysis in Table 4 shows that increasing k_t by 20% produces a 7% reduction in the fitted parameter S. The conclusion is that the error in the estimation of k_t based on Eq. (8) does not have large impact on the estimation of S.

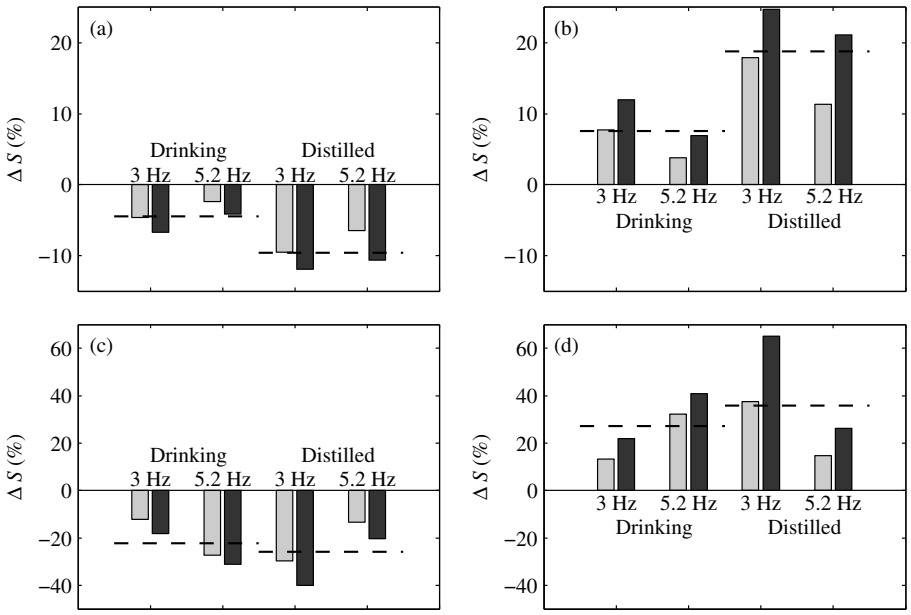

Fig. 8. Results of the sensitivity analysis, $\Delta S = 100(S^* - S)/S$, where S^* = fitted coefficient S with $k_t^* = k_t(1 + \Delta k_t/100)$ and $r_w^* = r_w(1 + \Delta r_w/100)$: (a) $\Delta k_t = 20\%$; (b) $\Delta k_t = -20\%$; (c) $\Delta r_w = 20\%$; (d) $\Delta r_w = -20\%$; light and dark gray bars = alternatives 1 and 2, respectively; dashed line = average

Discussion

This article states that DO consumption in benthic chambers depends on biochemical processes in sediments, S, water column, r_w, and turbulent mixing, k_t. Whereas the values of r_w and k_t are controlled by the particular conditions inside the benthic chamber, the coefficient S can be used to understand DO in sediment in the field. Once S was obtained based on the proposed method, k_t was estimated for field conditions using the expressions proposed by Dade (1993), Steinberger and Hondzo (1999), and Hondzo et al. (2005). In addition, the value of J was computed with Eq. (2). Hence, the rate of DO diffusion from sediments was related to the localized biochemical features of the sediments and to the particular hydrodynamic conditions of the study site.

The proposed methodology uses an expression for computing J given in Eq. (2). However, this equation contains several simplifications. From a biochemical standpoint, Eq. (2) was derived by considering a constant and homogeneous S in the sediments whose values do not depend on DO concentration in the water column. This simplification is based on early observations of Kühl and Jørgensen (1992), Rasmussen and Jørgensen (1992), and others. Microprofile measurements shown in Fig. 4 also support this assumption. Notice that the DO concentrations in the sediments vary between 0 and DO at the WSI (approximately 5 $gO_2\,m^{-3}$; see Fig. 4). Furthermore, the good fitting of Eqs. (4) and (6) with experiments 1, 2, and 4 (Fig. 7) validates the use of this equation to compute J, with DO concentrations inside the benthic chamber between 0 and 7 $(gO_2\,m^{-3})$. This conclusion cannot be directly extended to any sediment sample, however, particularly because biological processes are altered for small DO concentrations [$\lesssim 2(gO_2\,m^{-3})$ (Nakamura and Stefan 1994; Glud et al. 2007]. In these cases, the proposed methodology should be used to fit two different coefficients S: one for measurements with $C < 2(gO_2\,m^{-3})$ and one for measurements with $C > 2(gO_2\,m^{-3})$.

The correlation of the fitted S in the benthic chamber and that in the microprofiles was good; however, the ratio between the coefficient S obtained in the benthic chamber and the coefficient S observed in the microprofiles was 1.4. This difference might have been due to bioturbation and bioirrigation (Violler et al. 2003; Berg et al. 2003), although no macrofauna were observed in the sediment sample. It might also have been because microprofiles describe localized conditions whereas the coefficient S fitted with DO observations in the benthic chamber integrates conditions in the planar area of exposed sediments. Roy et al. (2005) studied the influence of sediment microtopography in the average diffusive flux and showed that the effective area of diffusive flux can be 10–20% larger than the flat area, thus reducing $h = VA^{-1}$ and modifying the value of all fitted parameters. For example, by increasing the surface area by 20% [$A' = 1.2A$, following the notation of Roy et al. (2005)], the fitted coefficients S match the microprofile observation. However, it is recommended that future applications use the geometric flat area of the sediments so that S includes microtopographic, bioturbation, and bioirrigation effects in J.

Water temperature varied in the benthic chamber according to air temperature. The standard deviation of diurnal oscillation reached 1.5°C in experiment 1 [Fig. 3(a)]. This oscillation influenced the value of biochemical parameters, particularly, S and r_w. To quantify this influence, two experiments without sediment were conducted with drinking water and $\omega = 3$ and 5.2 Hz, respectively. DO inside the benthic chamber decreased according to r_w [Eq. (3), with $J = 0$]. Figs. 9(a–d) show these measurements. The gray lines in Figs. 9(c and d) were obtained with the linear fit of the DO time series ($r^2 = 0.991$ and 0.997 for $\omega = 3$ and 5.2 Hz, respectively). These values indicate that a constant r_w is a reasonably good approximation. Despite this preliminary observation, the rate of DO consumption did vary with T. Fig. 9(e) shows $r_w(T)$, which was computed using the slope of the linear fit of two hours of measurements. The curve $r_w(T) = r_w(20)\theta^{T-20}$ was fitted with these observations, obtaining $\theta = 1.089 \pm 0.042$ and $r_w(20) = 1.307 \pm 0.288(gO_2\,m^{-3}\,d^{-1})$. For sediment oxygen demand, $\theta = 1.08$ is expected (Jørgensen and Bendoricchio 2001). Finally, the influence of water temperature can be included in alternative 1 [Eq. (4)] by assuming $S(T) = S_{20}\theta^{T-20}$, where S_{20} = the coefficient to fit, T = the observed water temperature,

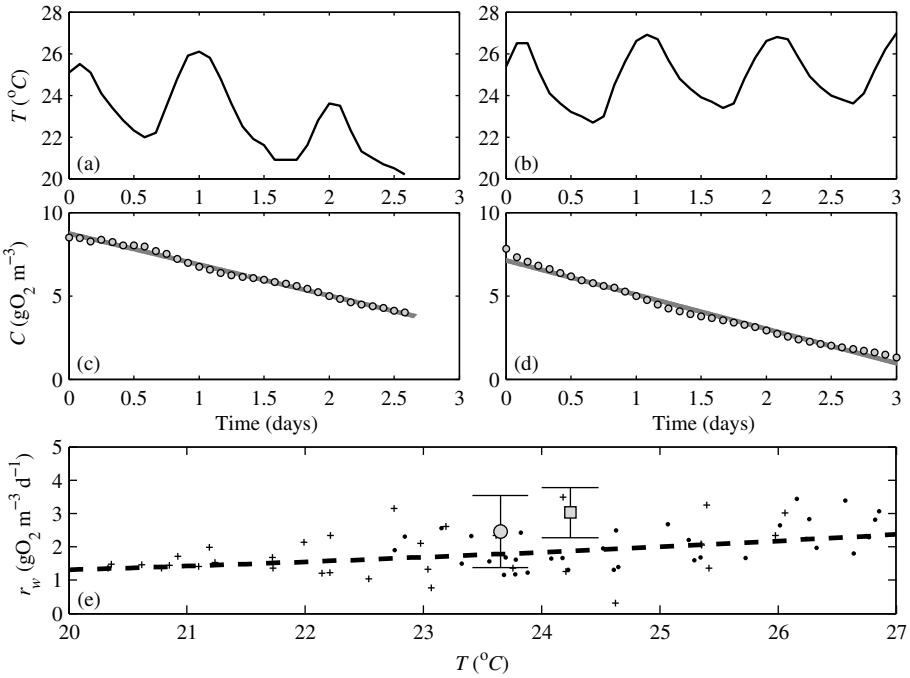

Fig. 9. Measured time series of water temperature (a and b) and DO (c and d) for experiments without sediments (gray line = fitted line for computing average r_w): (a and c) experiment with $\omega = 3$ Hz; (b and c) experiment with $\omega = 5.2$ Hz; (e) comparison of observed r_w as a function of water temperature for $\omega = 3$ Hz (pluses) and $\omega = 5.2$ Hz (black dots) [dashed line = fitted curve $r_w(T) = r_w(20)\theta^{T-20}$ ($\theta = 1.089 \pm 0.042$ and $r_w(20) = 1.307 \pm 0.288 (\mathrm{gO_2\ m^{-3}\ d^{-1}})$; gray circles and squares = averaged r_w fitted with sediments and drinking and distilled water, respectively]

and $\theta = 1.08$ (Jørgensen and Bendoricchio 2001). With the fitted S_{20}, the difference between the fitted coefficients in Table 3 and the temporal average of $S(T) = S_{20}\theta^{T-20}$ was smaller than 9%. The determination coefficients did not change with respect to the values shown in Table 4. In summary, even though there were water temperature changes in time, neglecting them was a good solution for this problem, and the fitted coefficients r_w and S were representative of the temporal average water temperature in the benthic chamber.

Some aspects of the biochemical processes related to DO consumption in sediments and water require further analysis. On the one hand, $r_w \neq 0$ was obtained in experiments 3 and 4 with distilled water, where DO consumption was not expected in the water column. The average r_w in drinking water was $2.46 (\mathrm{gO_2\ m^{-3}\ d^{-1}})$ and in distilled water was $3.03 (\mathrm{gO_2\ m^{-3}\ d^{-1}})$—approximately 50% higher than what was observed in experiments without sediments [the gray squares and circles in Fig. 9(e)]. Thus, it is hypothesized that the value of r_w is influenced by diffusive processes from the sediments to the water, but detailed studies are required to validate this. The observed S in distilled water was twice as large as that in drinking water, which indicates that S depends on the water quality in the benthic chamber. Further studies are required to define this interaction.

In conclusion, DO time series in a benthic chamber should not be used directly to understand DO consumption in the field. The methodology proposed here enables the analysis of benthic chamber measurements without the influence of flow conditions inside the apparatus.

Acknowledgments

This article was financed by the project Iniciación Fondecyt no. 11100306 and project Fondecyt Regular no. 1140821. In addition, the author wishes to thank the reviewers of this article for their constructive comments, Rodrigo Pérez and María del Mar Bustos for conducting the experiments, and Carolina Meruane for providing useful comments on an early version of the manuscript.

References

Arega, F., and Lee, J. (2005). "Diffusional mass transfer at sediment-water interface of cylindrical sediment oxygen demand chamber." *J. Environ. Eng.*, 10.1061/(ASCE)0733-9372(2005)131:5(755), 755–766.

Berg, P., et al. (2003). "Oxygen uptake by aquatic sediments measured with a novel non-invasive eddy-correlation technique." *Mar. Ecol. Prog. Ser.*, 261, 75–83.

Berg, P., Risgaard-Petersen, N., and Rysgaard, S. (1998). "Interpretation of measured concentration profiles in sediment pore water." *Limnol. Oceanogr.* 43(7), 1500–1510.

Bouldin, D. R. (1968). "Methods for describing the diffusion of oxygen and other mobile constituents across the mud-water interface." *J. Ecol.*, 56(1), 77–87.

Bryant, L., McGinnis, D., Larrai, C., Brand, A., Little, J., and Wüest, A. (2010). "Evaluating oxygen fluxes using microprofiles from both sides of the sediment-water interface." *Limnol. Oceanogr. Methods*, 8, 610–627.

Cole, T. M., and Buchak, E. M. (1995). *CE-QUAL-W2: A two-dimensional, laterally averaged, hydrodynamic and water quality model, version 2.0. user manual*, U.S. Army Corps of Engineers.

Dade, W. B. (1993). "Near-bed turbulence and hydrodynamic control of diffusional mass transfer at the sea floor." *Limnol. Oceanogr.*, 38(1), 52–69.

Dade, W. B., Hogg, A. J., and Boudreau, B. P. (2001). "Physics of flow above the sediment-water interface." *Fluid mechanics of environmental interfaces*, C. Gualtieri and D. T. Mihailovic, eds., Oxford University Press, New York, 4–43.

de la Fuente, A. (2014). "Heat and dissolved oxygen exchanges between the sediment and water column in a shallow salty lagoon." *J. Geophys. Res. Biogeosci.*, 119(4), 596–613.

Ferrón, S., et al. (2008). "Hydrodynamic characterization and performance of an autonomous benthic chamber for use in coastal systems." *Limnol. Oceanogr. Methods*, 6, 558–571.

Gao, K., Xu, J., Zheng, Y., and Ke, C. (2012). "Measurement of benthic photosynthesis and calcification in flowing-through seawater with stable carbonate chemistry." *Limnol. Oceanogr. Methods*, 10, 555–559.

Gin, K., and Gopalakrishnan, A. (2010). "Sediment oxygen demand and nutrient fluxes for a tropical reservoir in Singapore." *J. Environ. Eng.*, 10.1061/(ASCE)EE.1943-7870.0000119, 78–85.

Glud, R., Berg, P., Fossing, H., and Jørgensen, B. B. (2007). "Effect of the diffusive boundary layer on benthic mineralization and O2 distribution: A theoretical model analysis." *Limnol. Oceanogr.*, 52(2), 547–557.

Guatieri, C., and Gualtieri, P. D. (2008). "Gas-transfer at unsheared free-surface." *Fluid mechanics of environmental interfaces*, C. Gualtieri and D. T. Mihailovic, eds., Oxford University Press, New York, 131–160.

Hall, P., Anderson, L., Rutgers, M., Sundby, B., and Westerlund, S. (1989). "Oxygen uptake kinetics in the benthic boundary layer." *Limnol. Oceanogr.*, 34(4), 734–746.

Herzfeld, M., Hamilton, D. P., and Douglas, G. B. (2001). "Comparison of a mechanistic sediment model and a water column for hindcasting oxygen decay in benthic chambers." *Ecol. Modell.*, 136(2–3), 255–267.

Hipsey, M. R., Antenucci, J. P., and Hamilton, D. P. (2014). "Computational aquatic ecosystem dynamic model: CAEDYM v3. V3.2 science manual." *Centre for Water Research Rep.*, Centre for Water Research, Univ. of Western Australia. Perth, Australia.

Hondzo, M., Feyaerts, T., Donovan, R., and O'Connor, B. L. (2005). "Universal scaling of dissolved oxygen distribution at the sediment-water interface: A power law." *Limnol. Oceanogr.*, 50(5), 1667–1676.

Inoue, T., and Nakamura, Y. (2011). "Effects of hydrodynamic conditions on DO transfer at a rough sediment surface." *J. Environ. Eng.*, 10.1061/(ASCE)EE.1943-7870.0000293, 28–37.

Jahnke, R. A., Nelson, J. R., Richards, M. E.,, Robertson, C. Y., Rao, A. M. F., and Jahnke, D. B. (2008). "Benthic primary productivity on the Georgia midcontinental shelf: Benthic flux measurements and high-resolution, continuous in situ PAR records." *J. Geophys. Res.*, 113(C8), 1–13.

Jørgensen, B., and Revsbech, N. (1985). "Diffusive boundary layers and the oxygen uptake of sediment and detritus." *Limnol. Oceanogr.*, 30(1), 111–122.

Jørgensen, B. B., and Des Marais, J. (1990). "The diffusive boundary layer of sediments: Oxygen microgradients over a microbial mat." *Limnol. Oceanogr.*, 35(6), 1343–1355.

Jørgensen, B. B., and Gundersen, J. K. (1990). "Microstructure of diffusive boundary layers and the oxygen uptake of the sea floor." *Nature*, 345(6276), 604–607.

Jørgensen, B. B., Revsbech, N. P., and Cohen, Y. (1983). "Photosynthesis and structure of benthic microbial mats: Microelectrode and SEM studies of four cyaniubacterial communities." *Limnol. Oceanogr.*, 28(6), 1075–1093.

Jørgensen, S., and Bendoricchio, G. (2001). *Fundamentals of ecological modeling*, Elsevier Science and Technology, Oxford, U.K.

Kemp, P., Cole, J., Sherr, B., and Sherr, E. (1993). *Handbook of methods in aquatic microbial ecology*, CRC Press, FL.

Kühl, M., and Jørgensen, B. B. (1992). "Microsensor measurements of sulfate reduction and sulfide oxidation in compact microbial communities of aerobic biofilms." *Appl. Environ. Microbiol.*, 58(4), 1164–1174.

Mackenthun, A., and Stefan, H. G. (1998). "Effect of flow velocity on sediment oxygen demand: Experiments." *J. Environ. Eng.*, 10.1061/(ASCE)0733-9372(1998)124:3(222), 222–230.

Nakamura, Y., and Stefan, H. G. (1994). "Effect of flow velocity on sediment oxygen demand: Theory." *J. Environ. Eng.*, 10.1061/(ASCE)0733-9372(1994)120:5(996), 996–1016.

O'Connor, B. L., and Hondzo, M. (2008). "Dissolved oxygen transfer to sediments by sweep and eject motion in aquatic environments." *Limnol. Oceanogr.*, 53(2), 566–578.

Odum, H. T. (1956). "Primary production in flowing waters." *Limnol. Oceanogr.*, 1(2), 102–117.

Ordoñez, C., Pérez, R., and de la Fuente, A. (2013). "Experimental study of flow and diffusional mass transfer coefficient across the water-sediment interface determined by wind blowing an extremely shallow lagoon." *35th IAHR World Congress*, International Association of Hydroenvironmental Research, Chengdu, China.

Rasmussen, H., and Jørgensen, B. B. (1992). "Microelectrode study of seasonal oxygen uptake in a coastal sediment: Role of molecular diffusion." *Mar. Ecol. Prog. Ser.*, 81(3), 289–303.

Revsbech, R. P., Jørgensen, B. B., and Blackburn, T. H. (1980a). "Oxygen in the sea bottom measured with a microelectrode." *Science*, 207(4437), 1355–1356.

Revsbech, R. P., Sorensen, J., Blackburn, T. H., and Lomholt, J. P. (1980b). "Distribution of oxygen in marine sediments measured with microelectrodes." *Limnol. Oceanogr.*, 25(3), 403–411.

Roy, H., Huettel, M., and Jørgensen, B. B. (2005). "The influence of topography on the functional exchange surface of marine soft sediments, assessed from sediment topography measured in situ." *Limnol. Oceanogr.*, 50(1), 106–112.

Ryther, J. H. (1956). "The measurement of primary production." *Limnol. Oceanogr.*, 1(2), 72–84.

Santschi, P. H., Bower, P., Nyffeler, U. P., Azevedo, A., and Broecker, W. S. (1983). "Estimates of the resistance to chemical transport posed by the deep-sea boundary layer." *Limnol. Oceanogr.*, 28(5), 899–912.

Seber, G., and Wild, C. (2003). *Nonlinear regression*, Wiley, New York.

Sommer, S., Türk, M., Kriwanek, S., and Pfannkuche, O. (2008). "Gas exchange system for extended in situ benthic chamber flux measurements under controlled oxygen conditions: First application–sea bed methane emission measurements at Captain Arutyunov mud volcano." *Limnol. Oceanogr. Methods*, 6, 23–33.

Steinberger, N., and Hondzo, M. (1999). "Diffusional mass transfer at sediment-water interface." *J. Environ. Eng.*, 10.1061/(ASCE)0733-9372(1999)125:2(192), 192–200.

Tengberg, A., Stahl, H., Müller, V., Arning, U., Andersson, H., and Hall, P. O. J. (2004). "Intercalibration of benthic flux chamber: I. Accuracy of flux measurements and influence of chamber hydrodynamics." *Prog. Oceanogr.*, 60(1), 1–28.

Viollier, E., et al. (2003). "Benthic biogeochemistry: State of the art technologies and guidelines for the future of in situ survey." *J. Exp. Mar. Biol. Ecol.*, 285–286, 5–31.

Wetzel, R. (2001). *Limnology*, 3rd Ed., Academic Press, San Diego.